Heterogeneity in α-synuclein fibril activity correlates to disease phenotypes in Lewy body dementia

Arpine Sokratian[1], Julia Ziaee[1], Kaela Kelly[1], Allison Chang[1], Nicole Bryant[1], Shijie Wang[1], Enquan Xu[1], Joshua Y. Li[1], Shih-Hsiu Wang[2,3], John Ervin[2,3], Sandip M. Swain[4], Rodger A. Liddle[4], Andrew B. West[1,2*]

[1] Duke Center for Neurodegeneration Research, Departments of Pharmacology and Cancer Biology,[2]Neurology, [3]Pathology, and [4]Medicine, Duke University, Durham, North Carolina, USA

*C.A. Information: Andrew.West@Duke.edu, 3 Genome Court, Durham, North Carolina, 27710 USA

Supplemental Figs and Legends

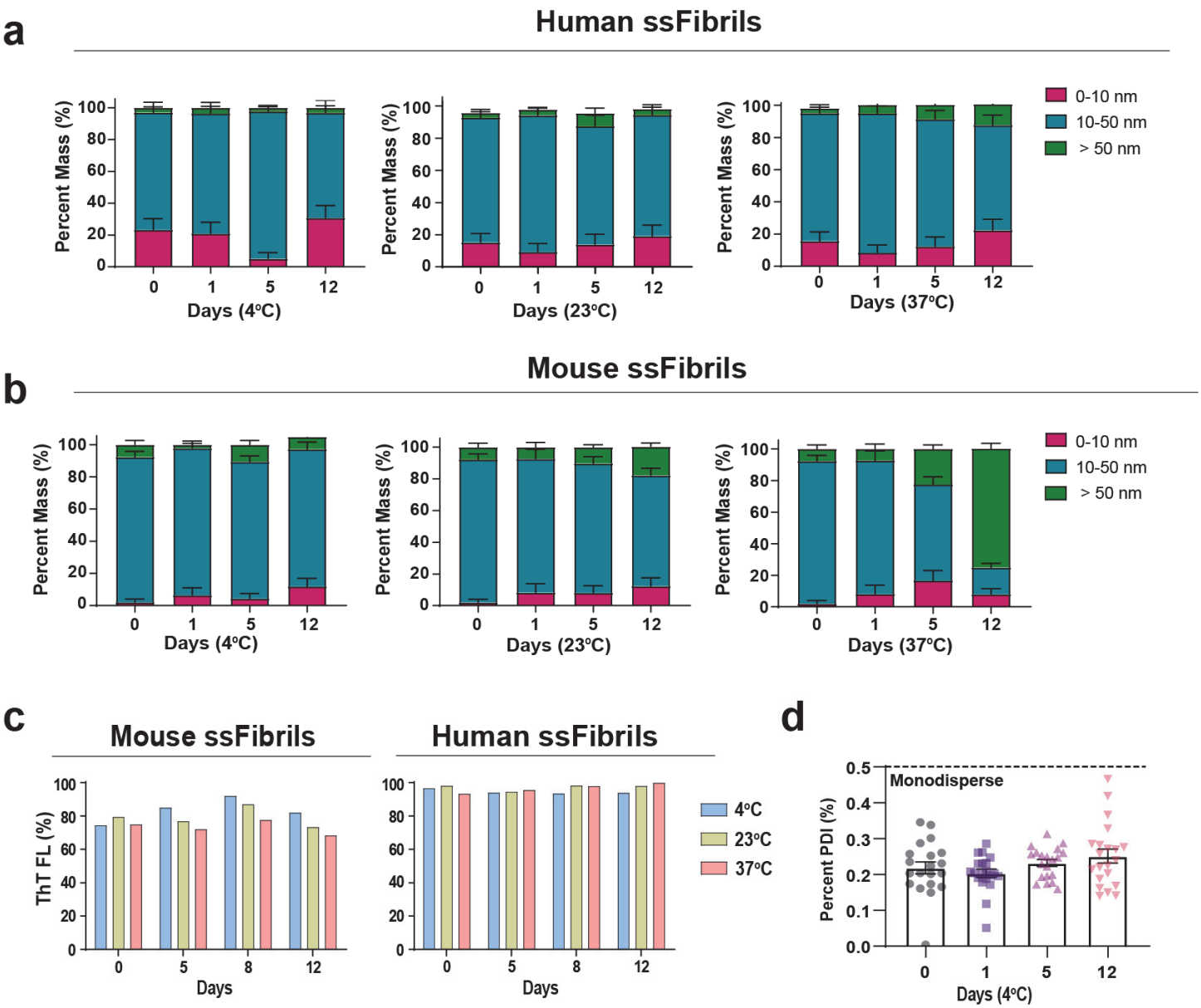

Supplemental Fig 1 High stability of ssFibrils with extended incubation and freeze-thaw cycling

Radius mass distributions measured by dynamic light scattering (DLS) for **a,** human, and **b,** mouse (α-synuclein) ssFibrils, assessed over twelve days of incubation at 4°C, 23°C, and 37°C. Only mouse ssFibrils demonstrated evidence of instability that occurred with aggregation to larger conformers at 37°C. No significant evidence of disaggregation was detected by DLS (i.e., monomeric species). **c** Thioflavin-T (ThT) endpoint fluorescence levels corresponding to mouse and human ssFibrils incubated over the indicated time (days) at three different temperatures (4°C, 23°C, 37°C). No condition was identified that resulted in a loss of ThT binding in the preparations. **d.** Polydispersity (PDI) measurements associated with human ssFibril preparations incubated at 4°C over twelve days. Size population uniformity is considered at PDI < 0.5. Errors bars represent standard error deviation of twenty individual acquisitions over three independent experiments.

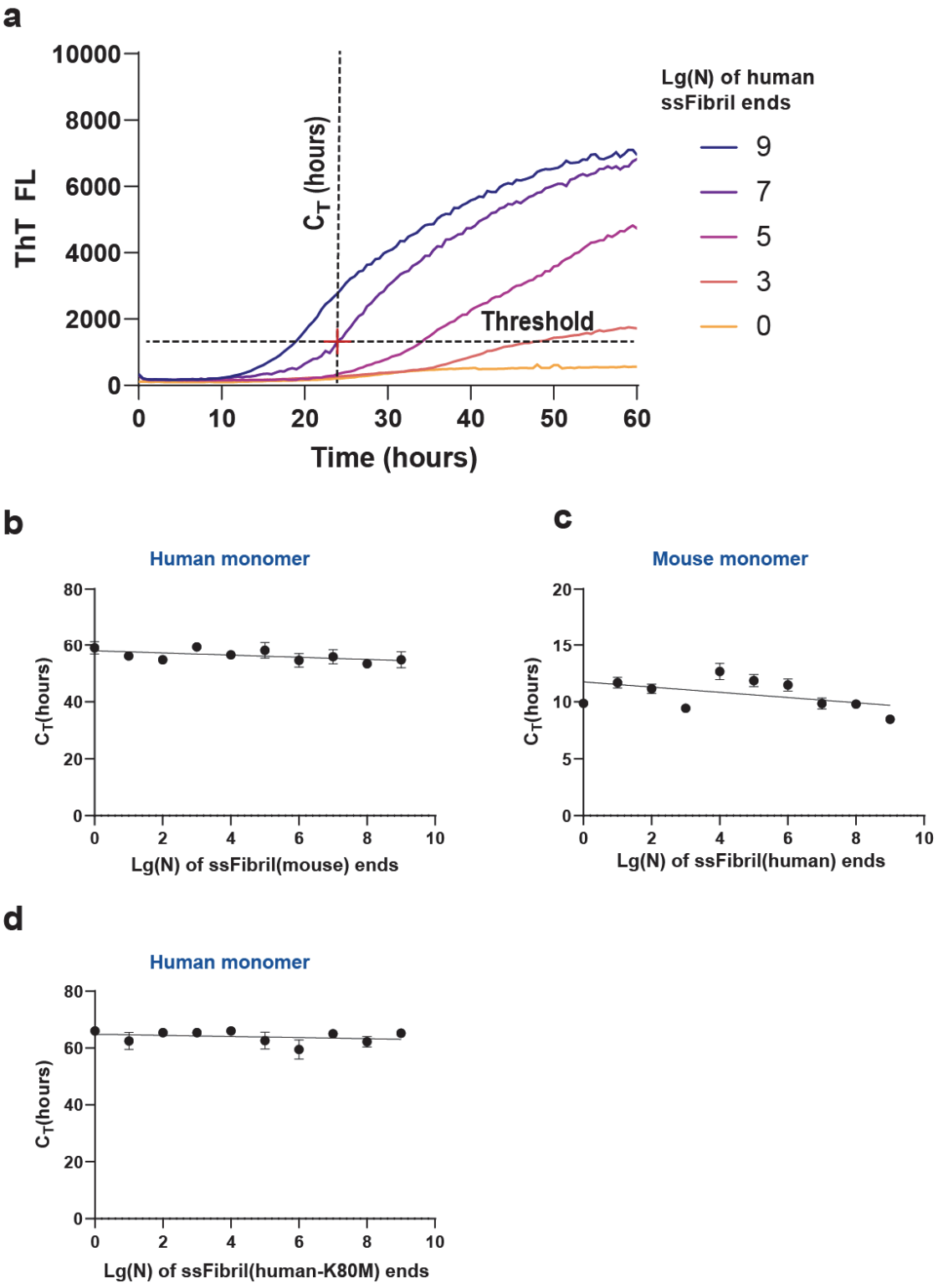

Supplemental Fig 2 qRT-QuIC performance and sequence-constrained specificity in determining fibril-forming units (FFUs).

a. Schematic diagram of a typical standard curve used to measure apparent fibril-forming units (FFUs). Standard curves are developed from triplicate reactions with spiked-in ssFibrils of known concentration, with

baseline measures for spontaneous fibrilization (Lg(0)) corresponding to reactions with no spiked in ssFibrils. Standard curves composed of ssFibrils of calculated concentrations of ssFibril ends are spiked into the same matrix that corresponds to experimental lysates, thus approximating the effects of buffers, detergents, and other protein and lipid constituents in standard curve reactions as experimental lysates. Thioflavin T fluorescent values, background subtracted, are exported into .CSV files analyzed via custom software to identify optimal threshold values across the standard curve. The threshold value is defined as the value that yields the highest possible correlation coefficient (i.e., closest to 1.0) across the known concentrations of ssFibril ends spiked into the reactions. This threshold is used to identify the C_T values (i.e., hours) for experimental lysates. When the r values of linear regression are higher than 0.9, the qRT-QuIC reaction is considered efficient with all ssFibril ends involved in ThT-monitored fibril formation in the reaction (one fibril forming unit is equivalent to one ssFibril end). Each Lg(N) curve is obtained through the calculation of mean values from three independent experiments (e.g., three wells of a 384-well plate). Error bars represent SEM, and dots indicate mean group values from the independent experiments. Each Lg(N) curve shown represents the average of three independent experiments. **c.** Poor qRT-QuIC performance (i.e., standard curve $r<0.8$) in optimal linear regression analysis based on C_T values of decadic logarithmic quantities of human monomer matched with mouse ssFibrils, or **c.** mouse monomer matched with human ssFibrils, or **d.** human monomer matched with human K80M-variant human ssFibrils. These results demonstrate high sequence constrained profiles associated with qRT-QuIC, where even a single amino acid substitution in α-synuclein can render the assay insensitive to exponentially increased possible ssFibril ends. All reactions shown in this figure were performed in phosphate saline at 37°C. Lg(0) represents spontaneous fibrilization under the indicated reaction conditions (i.e., the indicated ssFibrils species and monomer species). Error bars represent SEM, dots indicate mean group values from three independent experiments.

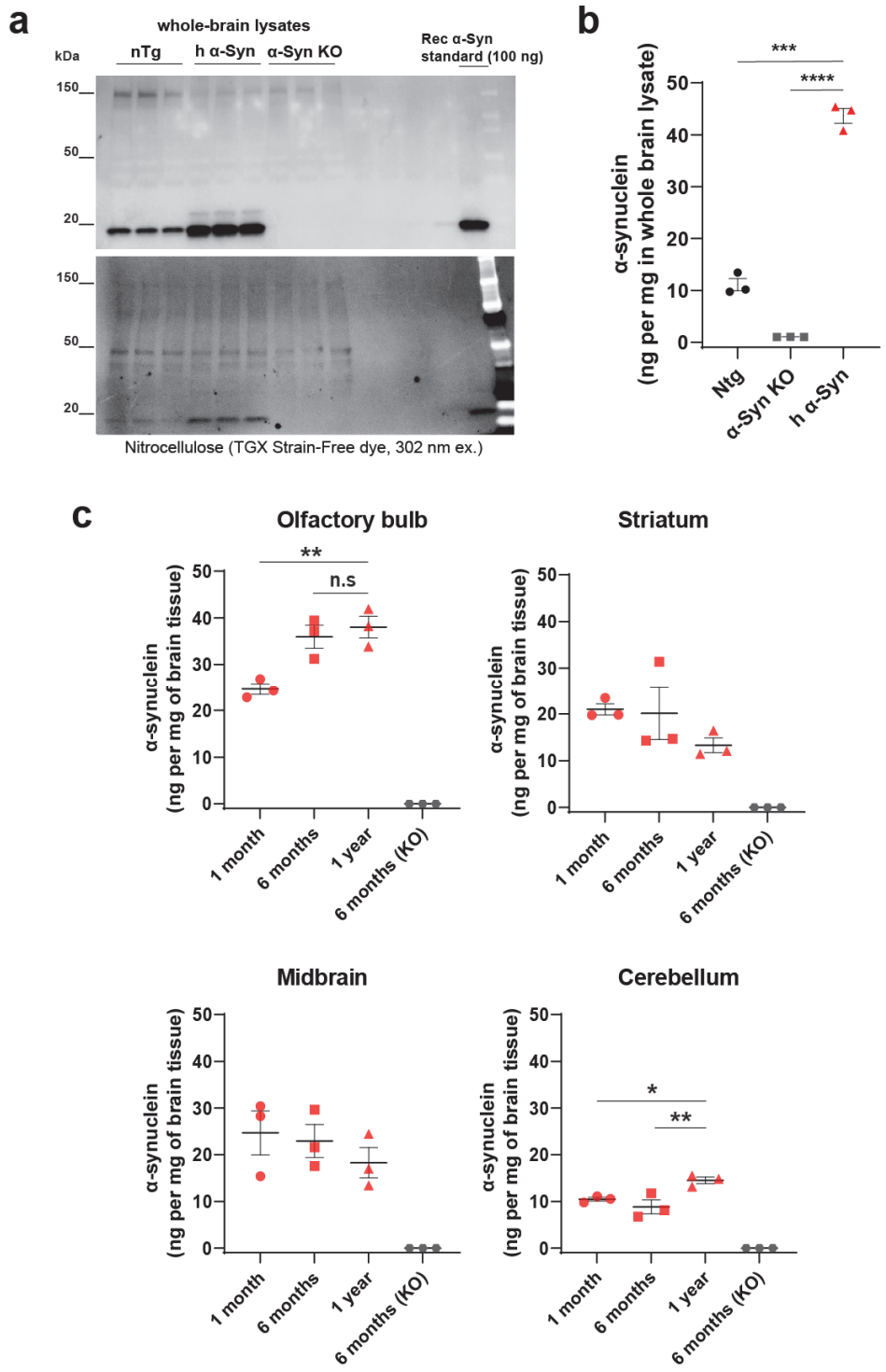

Supplemental Figure 3. Elevated α-synuclein expression in WT-hPAC-α-synuclein compared to non-transgenic and α-synuclein knockout (KO) mice

a. Representative immunoblots of triton X-100 solubilized α-synuclein from whole brain homogenates from non-transgenic (nTg), humanized α-synuclein mice (WT-hPAC-α-synuclein/m-α-synuclein KO), and α-synuclein KO mice, all at one-year of age (n=3 mice per group). Monomeric human α-synuclein protein standard was assigned for quantification of α-synuclein concentrations, with total lysate concentration of protein determined by BCA assay, equal amounts of protein loaded per lane, and stain-free membrane

analysis (shown at Ex. 302 nm together with α-synuclein) for total protein on the membrane to ensure equivalent transfer of proteins to membranes (see Methods). **b.** Calculated concentration of triton X-100 solubilized α-synuclein determined from whole brain extracts (normalized to weight/volume), or **c.** of the olfactory bulb, striatum, midbrain, and cerebellum of one-year, six-month, and one-month old humanized α-synuclein mice (N=9, equal number of males and females). Bars in each group column for panels in b and c represent mean values from the analysis of n=3 mice per group. Analysis was performed with one-way ANOVA and Holm-Sidak's multiple comparison test (with respect to one-year old humanized α-synuclein mice). n.s. is not significant, *$p<0.05$, **$p<0.01$.

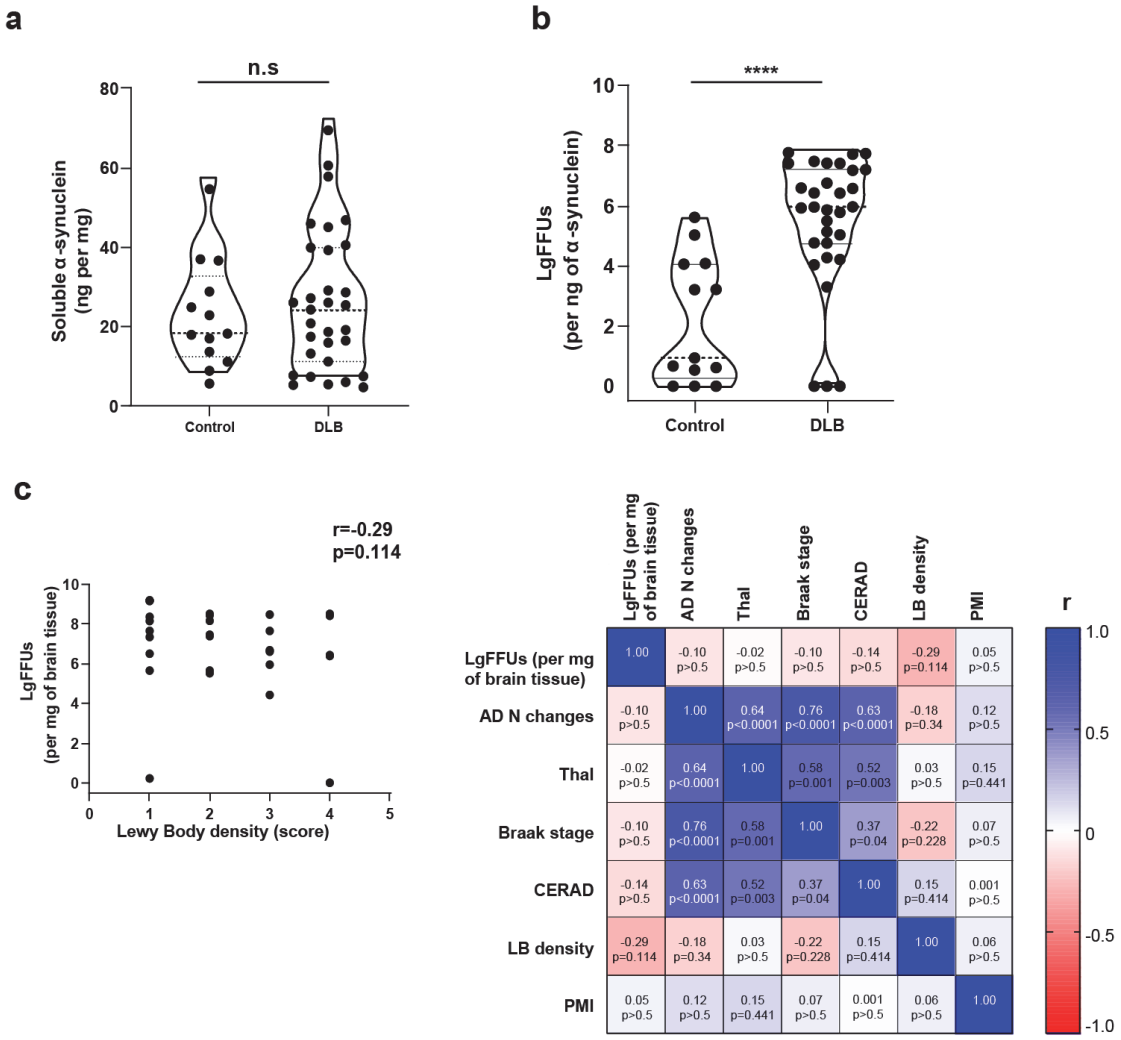

Supplemental Fig 4 Association between fibril-forming units (FFUs) in DLB brain tissue extracts and pathological features

a. Violin plots representing calculated concentrations in DLB and control groups of triton X-100 solubilized α-synuclein, where solubilized α-synuclein is expressed as nanograms per mg of brain tissue. Group comparisons were performed using unpaired t tests, and resultant p values are indicated. **b.** Quantification of FFUs normalized to the concentration of α-synuclein in brain tissue extracts from subjects with a pathological and clinical diagnosis of neocortical-type Lewy body dementia (Table 1) and neurologically normal control brain tissues, with spike-in standards of ssFibrils into α-synuclein KO brain extracts (see Supplemental Fig 3) for generation of standard curves. **c.** Left: Correlation analysis of LgFFUs per mg of brain tissue to Lewy Body density score in the neocortex. Right: Heat-map of correlation analysis of pathological parameters (from left to right: AD neuropathological change, TAP (Thal Aβ phase), tau Braak stage, and CERAD (Consortium to Establish a Registry for Alzheimer's Disease), LB density (Lewy body density), PMI (post-mortem interval), and LgFFUs per mg of brain tissue. Spearman correlation analysis was selected for the categorical variables, and corresponding r and p values are indicated. Each data point in the column plots in panels a and b represent a unique subject with the mean value calculated from at least three independent experiments for each subject.

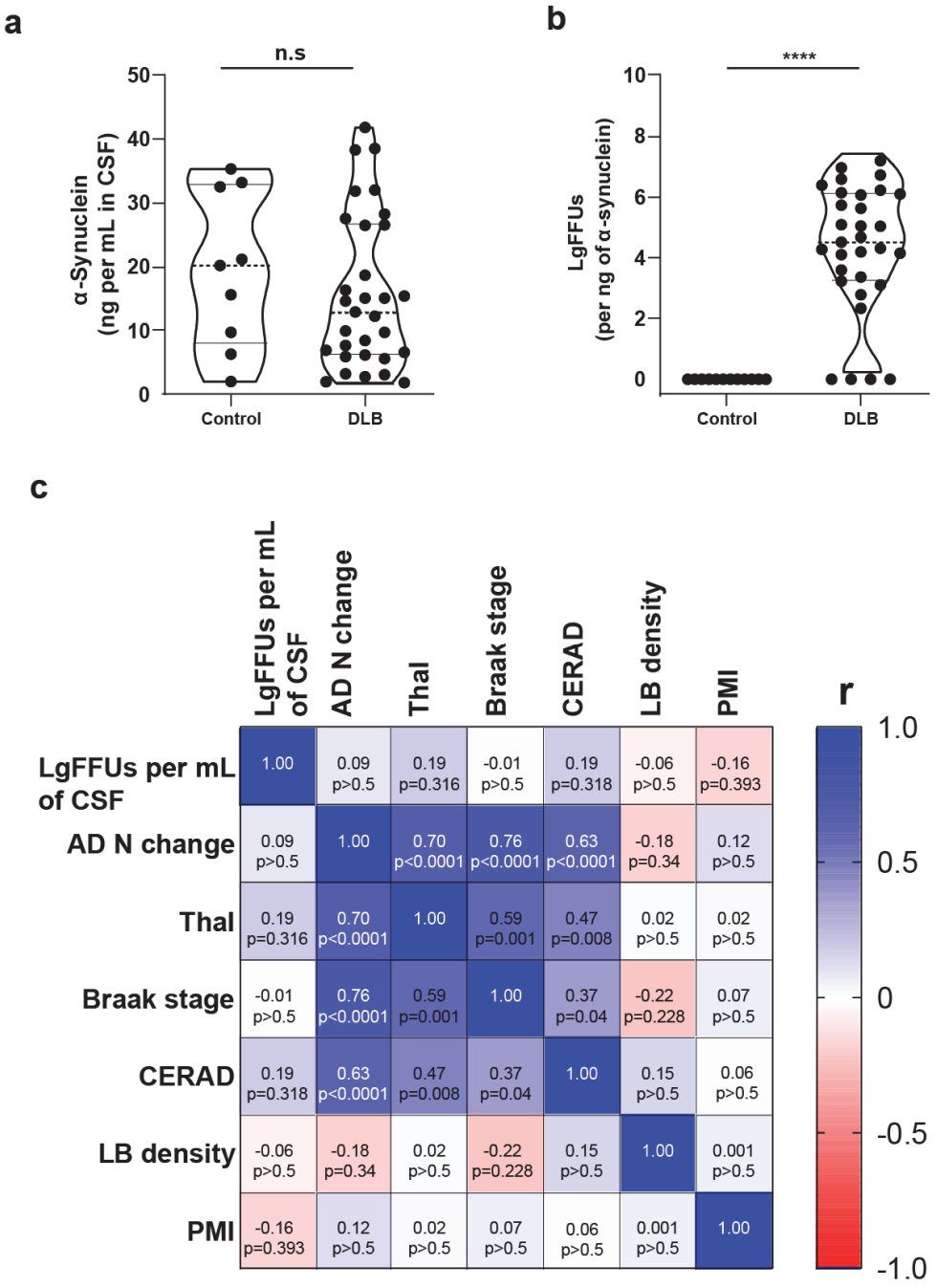

Supplemental Fig 5 Association between fibril-forming units (FFUs) in ventricular CSF and pathological features

a. Violin plots of the concentration of α-synuclein, expressed as ng of measured total α-synuclein (ELISA) per mL of CSF, in DLB and control groups. ELISA assay is a chemiluminescent-based ultra-sensitive assay using standard curves of recombinant α-synuclein standards (monomeric protein generated in-house) with r > 0.9 to ~10 pg per mL. **b.** Quantification of FFUs per ng of α-synuclein (volume adjusted) in brain-matched CSF from subjects with a pathological diagnosis of neocortical DLB (Table 1), with spike-in standards of ssFibrils into human control CSF previously identified as negative for α-synuclein fibril activity. Each data point represents the mean value calculated from at least three independent experiments from unique subjects. Comparative

group analysis was performed using a two-tailed unpaired t test. n.s. indicates not-significant, and **** indicating $p<0.00001$. **c.** Heat-map of correlation analysis of pathological parameters, with AD neuropathological change, TAP (Thal Aβ phase), tau Braak stage, and CERAD (Consortium to Establish a Registry for Alzheimer's Disease), LB density (Lewy body density), PMI (post-mortem interval), and LgFFUs per mL of CSF. Spearman correlation analysis was selected for the categorical variables, and corresponding r and p values are indicated. Each data point in the column plots in panels a and b represent a unique subject with the mean value calculated from at least three independent experiments for each subject.

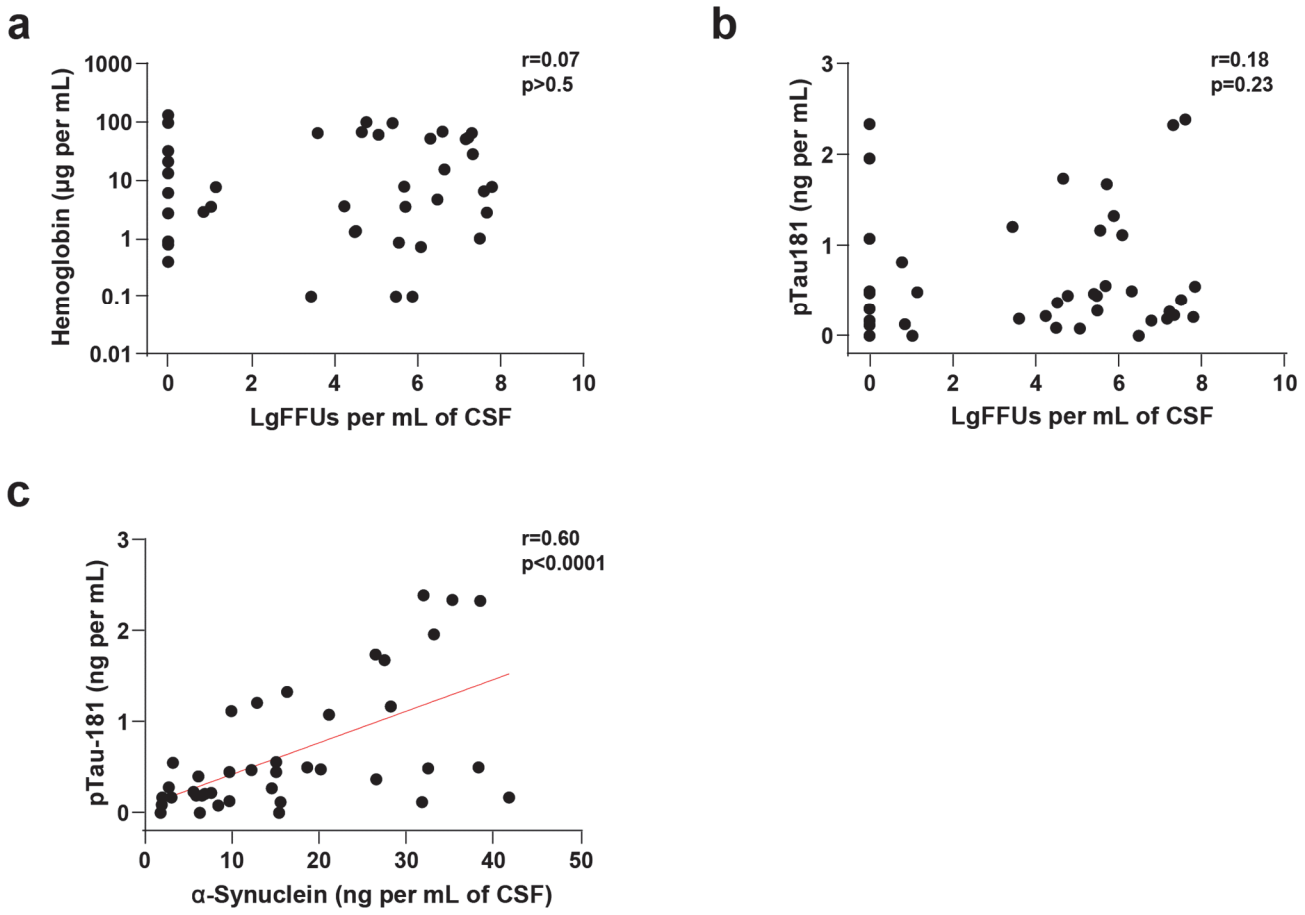

Supplemental Fig 6 Blood contamination and phospho-Tau concentrations in CSF do not correlate with measured α-synuclein fibril forming units (FFUs)

a. Scatterplots dot-plots evaluating the correlation strength between fibril-forming units (FFUs) and measured hemoglobin in the ventricular CSF. Hemoglobin concentrations were determined by ELISA analysis. **b.** phospho-Tau181 concentrations, expressed as ng per mL of CSF, were determined by single-molecule detection assay (SiMOA) and compared to calculated α-synuclein FFUs. From these analyses, neither pTau181 levels nor hemoglobin levels in the CSF appeared to interact with measured FFUs in the same CSF samples. **c.** In contrast, a correlation (positive) between pTau181 and total α-synuclein (ng per mL in CSF as determined by ELISA) was noted in both CSF samples from DLB cases and controls. Spearman coefficients and corresponding p values are indicated for all graphs. Each datapoint represents the mean value calculated from at least three independent measurements from each subject.

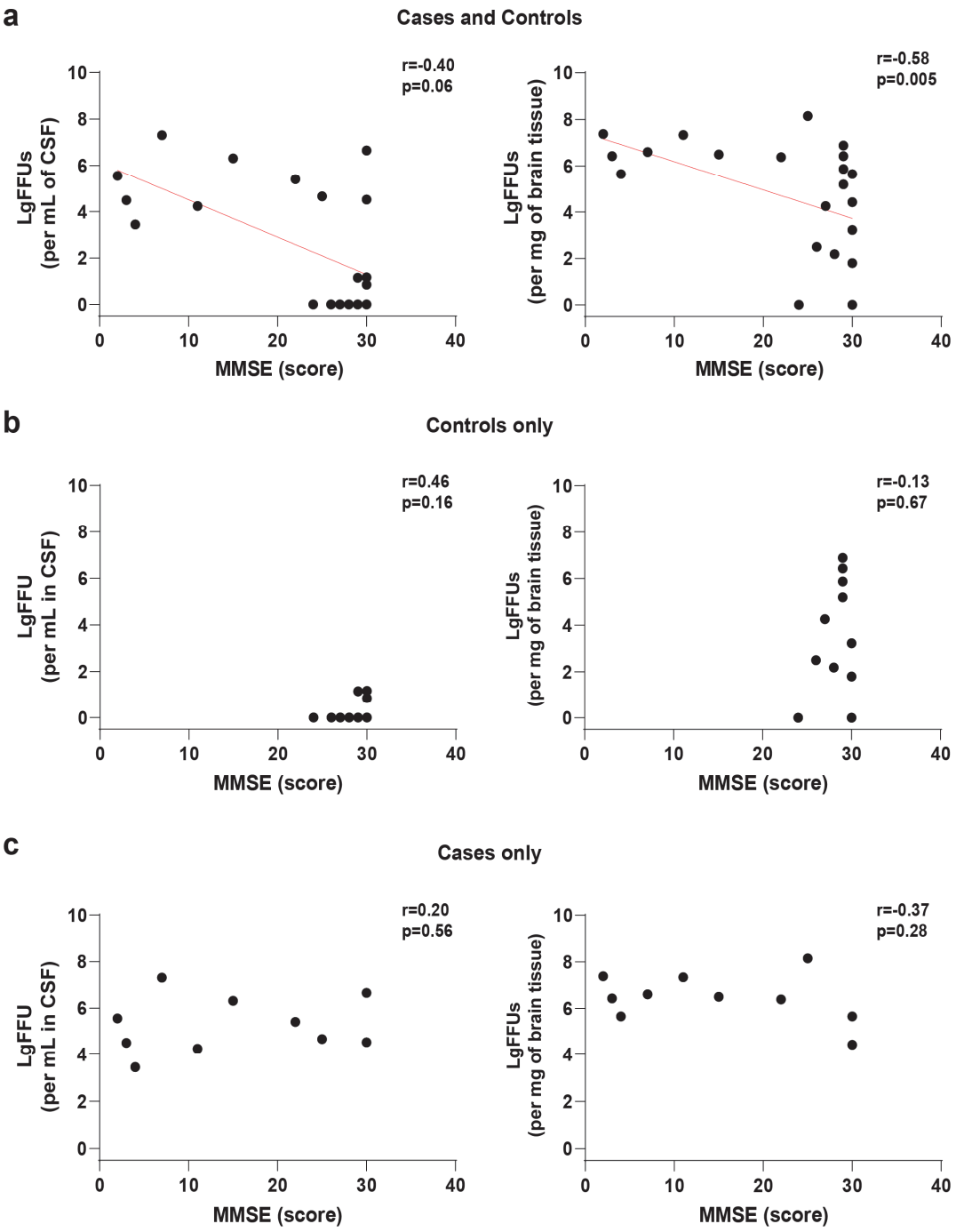

Supplemental Fig 7 Association between Mini-Mental State Examination (MMSE) score and LgFFUs in CSF and brain tissue

a. Correlation analysis of MMSE scores in cases and controls (10 scores available for DLB cases analyzed in this study and 13 available for control neurologically normal subjects, 2.3 yrs ± 0.69 (SEM) on average from MMSE to death for cases and controls) and LgFFUs (per mL) in CSF or brain homogenates (per mg of brain tissue), or **b.** controls only, or **c.** cases only. Nonparametric Spearman coefficients and corresponding p values are indicated.

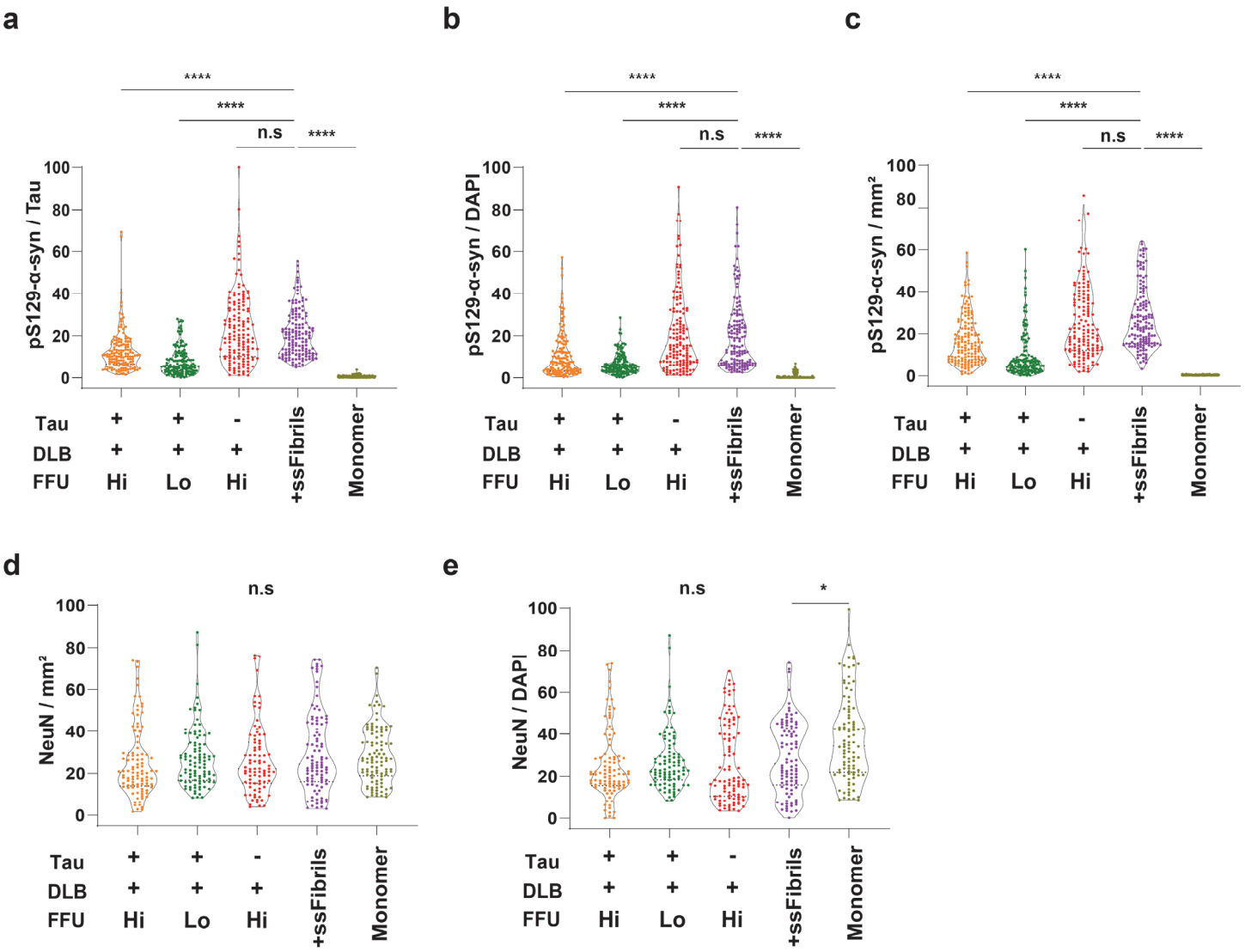

Supplemental Fig 8 Primary neuron cell viability measures after ssFibril treatment, and raw data corresponding to inclusion measurements

a. Violin plots of pS129-α-synuclein occupancy normalized to percent of tau occupancy in fluorescent photomicrographs of fixed primary hippocampal neuronal cultures from humanized α-synuclein mice, 10-days (days-in-vitro, DIV17) after ssFibril addition. 0.65 nM ssFibrils particles were added at DIV7, or monomer control, as indicated. **b.** pS129-α-synuclein occupancy in the photomicrographs normalized to the number of distinct DAPI spots (i.e., nuclei), or **c.** pS129-α-synuclein occupancy normalized to mm^2 area of the culture wells. **d.** Analysis of NeuN-positive nuclei abundancy in primary hippocampal neuronal culture wells from humanized α-synuclein mice, 17-days (DIV24) after ssFibril addition (0.65 nM ssFibrils particles were added at DIV7), and monomer control or **e**. NeuN-positive nuclei abundancy normalized to DAPI- spots. Each spot represents a unique non-overlapping image curated from at least six different wells of neurons from three different litters of humanized α-synuclein mice (for panels a, b, c) or two different litters (for panels d and e).

Significance is assessed by Kruskal-Wallis test with Dunn's multiple comparison post-hoc test (all groups compared to ssFibrils), and p values are indicated where n.s. is not-significant, *p<0.1, ****p<0.0001.